Integral action with time scale separation: A mechanism for modularity in biological systems

Integral Action with Time Scale Separation: A Mechanism for Modularity in Biological Systems

Phillip Rivera-Ortiz[1] and Domitilla Del Vecchio[1] *IEEE Member*

***Abstract*— Modularity is the property according to which the input/output dynamic behavior of a system does not appreciably change after interconnection with other systems. Whether modularity is a natural property of biological systems is one of the most vexing questions in systems biology and crucial for the advancement of synthetic biology. In this paper, we recall design techniques for disturbance attenuation, which are well established in the control theory literature, and illustrate how the underlying principles are also found in biological systems as means to attain modularity. The specific system structure that we consider is the one where an integral action and the system internal dynamics occur at a much faster time scale than the reference input and external disturbances. In this case, the system displays a separation of time scales and can be taken to standard singular perturbation form to show that on the timescale of the reference input the effect of the disturbance is attenuated. We illustrate how this fast integral action structure is found in some interconnected biomolecular systems, where it allows to track time-varying input stimuli while rejecting loading disturbances due to interconnection with other systems.**

I. Introduction

Determining design techniques that render the input/output dynamic behavior of a system robust to uncertainty, arising, for example, from poorly known parameters, noise, and external disturbances, has been a major research focus in control theory [1], [2], [3], [4], [5]. Problems of disturbance rejection or decoupling and disturbance attenuation have been subject of intense research. Integral control is a specific instance of disturbance attenuation for the case in which reference and disturbance are constant. It has been demonstrated that important cellular functions such as sensing and moving toward environmental nutrients are naturally robust because their molecular circuitry implements an integral action [6]. This discovery suggests that natural systems have already been implementing design techniques that control engineers have developed for creating robust human-made systems. Therefore, we may be able to shed new light on biological principles for robustness to a number of different perturbations by leveraging the rich set of techniques of control theory.

In this paper, we address the modularity question in biological systems, that is, what mechanisms are in place to make the input/output dynamic behavior of a biological module robust to interconnection with other modules. It has been argued that modularity may be one of the natural principles of biological organization, making biology close to synthetic disciplines such as engineering and computer science [7], [8], [9]. As a consequence a modular approach to analysis and design, which proved essential in engineering, may be viable to untangle the complexity of biological systems and to engineer new ones [10].

It has been theoretically shown and also experimentally reported that typical biological modules, such as those incorporating protein-protein interaction circuits (phosphorylation) and/or gene regulation circuits, are subject to loading-like effects when they are interconnected with each other [11], [12], [13], [14], [15]. These effects have been called retroactivity, to extend the notion of loading to biological systems, and they can have severe effects on a system's input/output dynamic behavior. Measures have been taken in the design of synthetic biological circuits in order to mitigate these effects, as theoretically illustrated in [11], [16] and experimentally demonstrated in [12], [14]. From a theoretical point of view, the problem of making a system robust to retroactivity can be formulated as a disturbance attenuation problem as illustrated in [16]. Here, the problem was solved by leveraging the interconnection structure typical of biological systems and employing time-scale separation as an equivalent mechanism for high-gain feedback in nonlinear systems [17].

In this paper, we analyze a typical structure of the interconnection between two biomolecular systems and demonstrate, by performing a suitable change of variables, that there is a "hidden" integral action. This integral action allows fast signal transduction systems to track time varying input stimuli that evolve on the slower timescale of gene expression in the presence of arbitrarily large retroactivity caused by load (disturbance) on the output. As a concrete example, we illustrate how this principle for retroactivity attenuation is implemented by a phosphorelay system, the YPD1/SKN7 system [18], which is a circuit found in the osmotic stress response system of eukaryotic cells and is in charge of transmitting information from outside the cell to gene expression. This phosphorelay system is inherently fast, and consists of a series of phosphorylation cascades which are able to track changes in the environment to drive a large number of DNA targets [19].

This paper is organized as follows. In Section II, we introduce a class of systems that implements disturbance attenuation through time scale separation and integral action.

[1]Department of Mechanical Engineering and the Laboratory of Information and Decision Systems, Massachusetts Institute of Technology, MA, 02139 USA e-mail: pmrivera@mit

This work was supported by AFOSR Grant # FA9550-12-1-0129 and NSF-CCF Award # 1058127

In Section III, we introduce the model of interconnected biological systems and show that this system incorporates an integral action. We then present a case study of retroactivity attenuation, the YPD1/SKN7 osmotic stress response pathway of yeast.

II. Integral action with time scale separation

In this paper, we consider systems in the form

$$\dot{r} = f_r(r,t) \tag{1}$$
$$\dot{d} = f_d(d,t) \tag{2}$$
$$\dot{z} = g_1(x_1,x_2,r,\beta) \tag{3}$$
$$\dot{x}_1 = g_2(x_1,x_2,r,\beta) + g_3(x_1,x_2,z,r,d) \tag{4}$$
$$\dot{x}_2 = f(x_1,x_2,z,r,d,\beta), \tag{5}$$

in which the functions f_r, f_d, g_i, f are smooth, $r \in \mathbb{R}^s$ is a time varying input and $d \in \mathbb{R}^q$ is a time varying disturbance, $(x_1, x_2) \in \mathbb{R}^n$ are the system states, $x_2 \in \mathbb{R}^p$ is the system output and $z \in \mathbb{R}^p$ is an integrator. We make the following assumptions.

- A1. There exists an $\alpha > 0$ such that $\|f_r(r,t)\| \leq \alpha$, $\|f_d(d,t)\| \leq \alpha$, $\|g_3(x_1,x_2,z,r,d)\| \leq \alpha$, for all (x_1,x_2,z,r,d,t).
- A2. We have $g_i(x_1,x_2,r,\beta) = \beta \bar{g}_i(x_1,x_2,r)$, for $i \in \{1,2\}$, $f(x_1,x_2,z,r,d,\beta) = \beta \bar{f}(x_1,x_2,z,r,d)$, and $g_3(x_1,x_2,r,d) = \alpha \bar{g}_3(x_1,x_2,r,d)$. $\bar{g}_i$ and $\bar{f}$ are independent of β and $\bar{g}_3$ is independent of α.
- A3. Let $(\bar{x}_1,\bar{x}_2,\bar{z}) = (\gamma_1(r),\gamma_2(r),\gamma_3(r,d)) =: \Gamma(r,d)$ be the equilibrium point of the boundary layer system

$$\begin{aligned} \frac{dz}{d\tau} &= \bar{g}_1(x_1,x_2,r) \\ \frac{dx_1}{d\tau} &= \bar{g}_2(x_1,x_2,r) \\ \frac{dx_2}{d\tau} &= \bar{f}(x_1,x_2,z,r,d) \end{aligned} \tag{6}$$

- A4. The Jacobian $A = \frac{\partial}{\partial x}\begin{pmatrix} \bar{g}_1(x_1,x_2,r) \\ \bar{g}_2(x_1,x_2,r) \\ \bar{f}(x_1,x_2,z,r,d) \end{pmatrix}$, where $x = (x_1,x_2,z)$ calculated at $x = \Gamma(r,d)$, has eigenvalues with strictly negative real parts, uniformly in (r,d).
- A5. The solution for (1)-(2) with $r(0) = r_0$, $d(0) = d_0$ exists and is unique for $t \in [0,T]$.

Theorem 1. *Consider system* (1)-(5) *and define* $\epsilon := \alpha/\beta$. *Then, under Assumptions A1 through A5 and further assuming that the initial condition* $(x_1(0),x_2(0),z(0))$ *belongs to the region of attraction of* $\Gamma(r(0),d(0))$, *for all* $t_b > 0$ *with* $t_b < T$ *there is* ϵ^* *such that for all* $\epsilon < \epsilon^*$

$$\|x_2(t) - \gamma_2(r(t))\| = O(\epsilon), \quad \text{for } t \in [t_b,T]. \tag{7}$$

Proof. Letting $\bar{t} := \alpha t$ be the normalized time and using Assumptions A1-A2, the closed loop system (1)-(5) can be re-written in the standard singular perturbation form [2]:

$$\begin{aligned} \dot{r} &= \bar{f}_r(r,t) \\ \dot{d} &= \bar{f}_d(d,t) \\ \epsilon \dot{z} &= \bar{g}_1(x_1,x_2,r) \\ \epsilon \dot{x}_1 &= \bar{g}_2(x_1,x_2,r) + \epsilon \bar{g}_3(x_1,x_2,z,r,d) \\ \epsilon \dot{x}_2 &= \bar{f}(x_1,x_2,z,r,d). \end{aligned} \tag{8}$$

in which with abuse of notation we have denoted $\dot{v} := dv/d\bar{t}$. By virtue of Assumptions A3-A5, we can apply Tikhonov's singular perturbation theorem on the finite time interval [3]. In particular by Assumptions A3-A4, it follows that $\bar{x}$ is also an exponentially stable equilibrium point of the boundary layer system described in A3 in which $\tau = \bar{t}/\epsilon$ is the normalized time and r and d are frozen at their initial conditions r_0 and d_0. Then, by Tikhonov's theorem and A5 it follows that for all $t_b > 0$ with $t_b < T$, there is $\epsilon^* > 0$ such that for all $\epsilon < \epsilon^*$ and $(x_1(0),x_2(0),z(0))$ inside the region of attraction of $\Gamma(r(0),d(0))$ we have

$$\|(x_1(t),x_2(t),z(t)) - \Gamma(r(t),d(t))\| = O(\epsilon),\ t \in [t_b,T]. \tag{9}$$

In particular, we have that $\|x_2(t) - \gamma_2(r(t))\| = O(\epsilon)$ for $t \in [t_b,T]$. □

When $\alpha \ll \beta$, vector fields whose norms are upper bounded by α represent dynamics that evolve on a slower timescale when compared to the dynamics of the other vector fields. As a consequence of Theorem 1, the output $x_2(t)$ approximately tracks the desired reference $\gamma_2(r(t))$ despite the presence of the disturbance $d(t)$. The tracking error becomes smaller as the disturbance and the reference input become slower compared to the system dynamics. Furthermore, the convergence to the desired trajectory becomes faster as the disturbance and reference trajectory become slower compared to the system dynamics. Therefore, we conclude that a system with the structure (1)-(5) can track a reference trajectory while attenuating disturbances when $\alpha \ll \beta$. Specifically, the key structural property that enables this ability is the combination of the integral action and internal dynamics that are much faster compared to the reference and disturbance dynamics.

A similar result is provided in [20] on the infinite time horizon when, additionally, the input and disturbance values are required to be bounded for all time. For the application considered here an infinite time horizon is not required, which allows us to place less stringent restrictions on the reference and disturbance.

In standard control design problems, the form of the function g_1 is designed such that the output tracks the desired reference trajectory and commonly $g_1(x_1,x_2,r,\beta) = \beta(r - x_2)$. Furthermore, functions g_2 and f result from a feedback control $u = K(x_1,x_2,z,r)$, designed such that the equilibrium point $(\bar{x}_1,\bar{x}_2,\bar{z}) = \Gamma(r,d)$ is exponentially stable, that is, A4 is satisfied. This feedback law can, under technical assumptions, also be designed such that the closed

loop system dynamics (3)-(5) are much faster compared to the inputs dynamics. For a detailed treatment on how to design the feedback map K in such a way that the closed loop dynamics of linear time invariant systems evolve on a much faster time scale than the input dynamics, the reader is referred to [17], [21], [22] and to the references therein. By contrast, as we will see in the next sections, in the case of biological systems, g_i and f are established by the structure of the biomolecular reactions and commonly are such that the equilibrium point $(\bar{x}_1, \bar{x}_2, \bar{z})$ is exponentially stable uniformly in (r, d). The parameter that can, to some extent, be designed by suitable choice of (amounts of) chemical species is the time scale ratio α/β.

A. Comparison with high gain feedback

Since only approximate tracking is reached when the reference and/or the disturbance are time-varying, a natural question is why it is useful to have an integral action as opposed to having just a high-gain feedback. In fact, high gain feedback can reach, under suitable technical assumptions, approximate tracking even in the presence of disturbances (see [21], [23], for example and the references therein). However, the control effort required to attenuate the effect of the disturbance may be substantially higher without an integral action. We illustrate this point through a simple example.

Consider the scalar system $\dot{x} = u + d(t)$, in which we have that the disturbance is time-varying but bounded by a known value D, that is, $|d(t)| \leq D$. We seek to design a feedback law $u = K(x, r)$ to have x track a constant reference input r. Let $K(x, r) = k(r - x)$ with $k > 0$, so that the closed loop system becomes

$$\dot{x} = k(r - x) + d(t). \tag{10}$$

Direct integration of this system along with the bound $|d(t)| \leq D$ leads to a steady state error upper bound $\|r(t) - x(t)\| \leq \frac{D}{k}$, as it is illustrated in the Appendix. Thus, to make the upper bound smaller than some value e, it is sufficient to have $k > D/e$, indicating that the control effort increases as the amplitude of the disturbance increases.

We now examine the situation in which we add an integral action $\dot{z} = 10k^2(r - x)$ and a stabilizing feedback law $K(x, r) = 11k(r - x) + z$, so that the system becomes

$$\begin{aligned} \dot{d} &= f_d(d, t) \\ \dot{z} &= 10k^2(r - x) \\ \dot{x} &= 11k(r - x) + z + d. \end{aligned} \tag{11}$$

The integrator dynamics $\dot{z}$ and feedback $K(x, r)$, were selected such that the closed loop system has eigenvalues $\lambda_1 = -k$, $\lambda_2 = -10k$, though this choice is arbitrary. In the case in which $|\bar{f}_d(d, t)| \leq \alpha$, we have that a steady state error upper bound is $\|r(t) - x(t)\| \leq \frac{\alpha}{9k^2}$, as it is illustrated in the Appendix. As a consequence, we can guarantee that the upper bound is less than e by having $k^2 > \alpha/(9e)$.

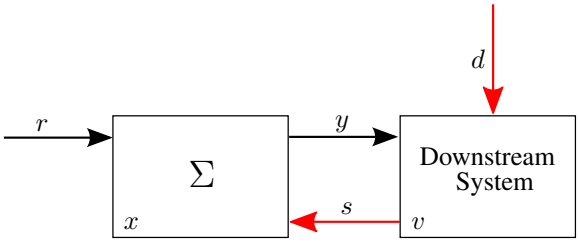

Fig. 1: System Σ with state x, reference input r, output y and retroactivity to the output s. The downstream system has state v and disturbance d.

Comparing this requirement with the requirement for the case of no integral action $k > D/e$, we note the following. When the disturbance amplitude is large but its derivative is small, the same tracking error upper bound can be achieved with a much lower feedback gain by employing an integral action.

This example illustrates that if the system internal dynamics are much faster than the rate of change of the disturbance, then a prefixed tracking error in the presence of arbitrarily large disturbances can be guaranteed with much lower control efforts by using an integral action. Hence, when a system can be designed such that its time scale is faster than that of the inputs (seen as constant in this example), an integral action provides an energetically advantageous design, leading to lower steady state control efforts than found in high gain feedback with no integral action. This fact is particularly important to note in view of the biological application, in which the presence of an integral action suggests that nature may have made design choices that minimize, to some extent, the required energy expenditure.

III. Interconnected biomolecular systems

In this section, we introduce a general system structure that characterizes biomolecular systems and their interconnections as illustrated in Fig. 1. Without loss of generality, we partition the state vector of system Σ into two parts and write $x = (x_1, x_2)$, in which $x_2 = y$ is the output of the system, that is, the vector of concentration of species that are involved in reactions with the downstream system. With this partition, the connected system takes the form:

$$\begin{aligned} \dot{r} &= f_r(r, t) \\ \dot{d} &= f_d(d, t) \\ \dot{x}_1 &= h_1(x_1, x_2, r) \\ \dot{x}_2 &= h_2(x_1, x_2, r) + Bs(x_2, d, v) \\ \dot{v} &= Ds(x_2, v, d), \end{aligned} \tag{12}$$

in which B and D are stoichiometry matrices [24], d is the vector of species (load) to which x_2 binds to form complexes v, and $s(x_2, v, d(t))$ is the retroactivity to the output [11]. It represents the reaction fluxes that affect the concentrations x_2 once the corresponding species are taken as an input to

the downstream system by binding to species d. Therefore, $d = 0$ implies $s(x_2, v, d) = 0$.

When the effects of retroactivity s are large, the behaviors of the isolated system Σ, given by $s = 0$, and that of the same system when connected are fairly different from each other [11], [16]. As a consequence, system Σ does not have the modularity property as its input/output dynamic behavior is influenced by its context, that is, by the systems it connects to. One natural question is whether nature has evolved mechanisms that allow system Σ to keep its isolated input/output dynamic behavior even when connected to downstream systems. In more technical terms, we are concerned with mechanisms for disturbance attenuation, where the disturbance to be attenuated is due to load $d(t)$.

Consider the form of the connected system (12). Assuming that the reactions between the upstream and downstream system species do not create or destroy molecules but only transform them (conservation of mass), we have that there is an invertible matrix T and a matrix P such that $TD + PB = 0$. Thus, we can define the change of variables $z = Tv + Px_2$ such that in the new variables (x_1, x_2, z) system (12) becomes

$$\begin{aligned} \dot{r} &= f_r(r,t) \\ \dot{d} &= f_d(d,t) \\ \dot{z} &= h_2(x_1, x_2, r) \\ \dot{x}_1 &= h_1(x_1, x_2, r) \\ \dot{x}_2 &= h_2(x_1, x_2, r) + Bs(x_2, T^{-1}(z - Px_2), d). \end{aligned} \tag{13}$$

The third equation of this system implements the integral action, that is, z is the integral of $h_2(x_1, x_2, r)$. System (13) has the structure of system (1)-(5), in which $g_1(x_1, x_2, r, \beta) = h_2(x_1, x_2, r)$, $g_2(x_1, x_2, r, \beta) + g_3(x_1, x_2, z, r, d) = h_1(x_1, x_2, r)$, and $f(x_1, x_2, z, r, d, \beta) = h_2(x_1, x_2, r) + Bs(x_2, T^{-1}(z - Px_2), d)$.

Biomolecular systems are characterized by several different time scales [25]. In particular, among the slowest processes there is gene expression (transcription and translation), with characteristic time scales ranging from minutes to hours depending on the organism. Signal transduction through protein covalent modification, including phosphorylation and phosphorelay systems, are faster, with characteristic time scales ranging from seconds to minutes [26]. On the fastest end of the time scale, there are molecule-molecule interactions, such as reversible binding, with characteristic times from subseconds to seconds [25]. Also, the rate of change of the input stimulus $r(t)$ can be very slow, such as in the case in which $r(t)$ represents the time-varying concentration of nutrients outside the cell, the day-light cycle, or other environmental molecules. This input is also fairly slow when resulting from gene expression processes, such as found in gene transcription networks. Thus, a question is whether interconnected natural systems, which commonly have the structure of system (12), display a slow/fast/slow pattern, in which the input $r(t)$ is slow, the system that transmits this signal to the output $x_2(t)$ is faster, and then the downstream system that receives this signal applies a load $d(t)$ that also changes slowly.

Interestingly, this pattern is fairly common. One example is provided by signal transduction networks, which are responsible for transmitting information from outside the cell down to gene expression. These networks are usually composed of fast modules, such as phosphorylation and phosphotransfer systems. These systems often have large amounts of downstream targets (load), including substrates and/or operator sites on the DNA, whose total concentration is about constant [24]. Going back to system (13), large amounts of downstream targets imply the term $Bs(x_2, T^{-1}(z - Px_2), d)$ is commonly very large. This further supports that the integral structure in system (13) is essential for attenuating the effect of s on the trajectory $x_2(t)$. In fact, the absence of the integral action would require much larger gains (very fast time scale for the (x_1, x_2) dynamics) to obtain the same tracking error. This is consistent with the fact that natural systems may have evolved to minimize energy consumption in normal working conditions [27].

It is known that many transcription regulators both in prokaryotes and eukaryotes undergo phosphorylation before regulating downstream DNA targets [28]. These fast phosphorylation modules are found between an upstream system with characteristic time scale of transcription/translation (slow) and a downstream system applying a constant load due to DNA binding sites. An example of this is the YPD1/SKN7 and YPD1/SSK1 phosphorylation pathways of the osmotic stress response in yeast which are reported to regulate many downstream clients through transcriptional activation [19]. This is the system on which we focus next.

A. A case study in retroactivity attenuation: The YPD1/SKN7 pathway

As a specific instance of system (12), we consider the YPD1/SKN7 phosphotransfer system, which is a building block of the osmotic stress sensor in *Saccharomyces cerevisiae* (yeast) [29]. We model this system employing biochemical parameter values inside their allowable physical range, and illustrate how both the integral action and separation of time scales naturally arise. Fig. 2 depicts the YPD1/SKN7 pathway.

We can write the considered chemical reactions using mass-action kinetics notation [24]. Specifically, species at the beginning of the arrows indicate the reactants, the value on top or bottom of the arrow indicate the production rate constant and the species at the end of the arrow are the reaction products. The considered reactions are the following. The production and decay of U are given by $\emptyset \xrightarrow{k(t)}$ U , U $\xrightarrow{\delta} \emptyset$ U* $\xrightarrow{\delta} \emptyset$. The phosphotransfer reactions are given by U $\underset{k'_p}{\overset{k_p}{\rightleftharpoons}}$

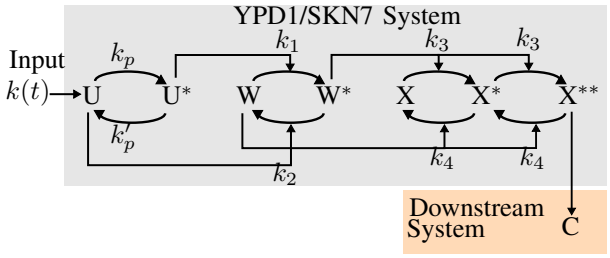

Fig. 2: This diagram shows the interconnection between species involved in the SKN7 activation pathway. The notation considered is: U represents a phosphate donor for YPD1, W represents protein YPD1, X represents protein SKN7, C represents the complex of SKN7 bound with the downstream system and the asterisk (*) represents the addition of phosphate groups. The system input given by k(t) results in the activation of SKN7 by the addition of two phosphate groups denoted as X**. Protein X** is the output of the YPD1/SKN7 pathway and it is used as an input to a downstream system.

U*, U*+W $\underset{k_2}{\overset{k_1}{\rightleftharpoons}}$ U+W*, X+W* $\underset{k_4}{\overset{k_3}{\rightleftharpoons}}$ X*+W, X*+W* $\underset{k_4}{\overset{k_3}{\rightleftharpoons}}$ X**+W [24]. The spontaneous dephosphorylation reactions are given by X* $\xrightarrow{k_5}$ X, X** $\xrightarrow{k_6}$ X*, W* $\xrightarrow{k_7}$ W. The binding reaction of X** with the DNA promoter binding sites p (load) is given by X**+p $\underset{k_{off}}{\overset{k_{on}}{\rightleftharpoons}}$ C. Defining $U_T := U + U^*$ we can write the ODE model given by these reactions as

$$\dot{U}_T = k(t) - \delta U_T \tag{14}$$

$$\dot{U}^* = -k_1 U^*(W_T - W^*) + k_2 W^*(U_T - U^*) + k_p(U_T - U^*) - k_p' U^* - \delta U^* \tag{15}$$

$$\dot{W}^* = k_1 U^*(W_T - W^*) - k_2 W^* U + k_4 X^*(W_T - W^*) - k_3 \left(X_T - X^* - X^{**} - C\right) W^* - k_3 X^* W^* + k_4 X^{**}(W_T - W^*) - k_7 W^* \tag{16}$$

$$\dot{X}^* = k_3 \left(X_T - X^* - X^{**} - C\right) W^* - k_4 X^*(W_T - W^*) - k_3 X^* W^* + k_4 X^{**}(W_T - W^*) - k_5 X^* + k_6 X^{**} \tag{17}$$

$$\dot{X}^{**} = k_3 X^* W^* - k_4 X^{**}(W_T - W^*) - k_6 X^{**} - k_{on} X^{**}(p_T - C) + k_{off} C \tag{18}$$

$$\dot{C} = k_{on} X^{**}(p_T - C) - k_{off} C \tag{19}$$

where the conservation laws $X_T = X + X^* + X^{**} + C$, $W_T = W + W^*$, $p_T = p + C$ were considered.

We can re-write this system in terms of normalized concentrations to elucidate the different reactions timescales. Let us define $u_T := \frac{U_T}{U_0}$, $u^* := \frac{U^*}{U_0}$, $w^* := \frac{W^*}{W_T}$, $x^* := \frac{X^*}{X_T}$, $x^{**} := \frac{X^{**}}{X_T}$ and $c := \frac{C}{p_T}$ in which U_0 is the maximal value reachable by U_T given by $U_0 := \max_t |k(t)|/\delta$. Let us define $\bar{k}(t) := k(t)/U_0$ and assume that $p_T/X_T \ll 1$. Note that even if $p_T/X_T \ll 1$, the retroactivity effect may be substantial because X^{**}, which is the species to which the load is applied, can be also much smaller than X_T. This assumption allows us to fit the structure of system (13) and further the system described in Theorem 1. This assumption may be relaxed as shown in [30] to obtain a similar tracking result. The system now becomes:

$$\dot{u}_T = \bar{k}(t) - \delta u_T \tag{20}$$

$$\dot{u}^* = -k_1 W_T u^*(1 - w^*) + k_2 W_T w^*(u_T - u^*) + k_p(u_T - u^*) - k_p' u^* - \delta u^* \tag{21}$$

$$\dot{w}^* = k_1 U_0 u^*(1 - w^*) - k_2 U_0 w^*(u_T - u^*) + k_4 X_T x^*(1 - w^*) - k_3 X_T \left(1 - x^* - x^{**}\right) w^* - k_3 X_T x^* w^* + k_4 X_T x^{**}(1 - w^*) - k_7 w^* \tag{22}$$

$$\dot{x}^* = k_3 W_T \left(1 - x^* - x^{**}\right) w^* - k_4 W_T x^*(1 - w^*) - k_3 W_T x^* w^* + k_4 W_T x^{**}(1 - w^*) - k_5 x^* + k_6 x^{**} \tag{23}$$

$$\dot{x}^{**} = k_3 W_T x^* w^* - k_4 W_T x^{**}(1 - w^*) - k_6 x^{**} - k_{on} p_T x^{**}(1 - c) + k_{off}(p_T/X_T) c \tag{24}$$

$$\dot{c} = k_{on} X_T x^{**}(1 - c) - k_{off} c. \tag{25}$$

The time scale of the first differential equation is determined by the decay rate $\delta \in [0.004, 0.01]$ min^{-1}[31] while the timescale of the remaining differential equations is faster and determined by phosphotransfer reactions. We can consider the reactions involving kinetic rates $\{k_p,\ k_1 W_T,\ k_2 W_T,\ k_3 W_T,\ k_4 W_T,\ k_6,\}$ as evolving in a fast timescale characterized by the phosphorylation rate $k_4 W_T \in [1, 600]$ min^{-1} [29]. The remaining phosphotransfer reactions are slower since $\{k_p', k_5, k_7\} \in [0.004, 1]$ min^{-1} [29], [32]. Furthermore, the binding/unbinding of x^{**} with DNA occurs at a maximum rate $k_{on} p_T \leq 0.13$ min^{-1} [33]. To demonstrate the hidden integral action, we will show how this system fits the structure given by (13), then apply Theorem 1 to obtain the desired tracking result.

First note that this system fits the structure of system (12), where $d = p_T$ is constant, $r = u_T$, $x_1 = (u^*, w^*, x^*)$, $x_2 = x^{**}$, $v = c$, $h_1(x_1, x_2, r(t))$ is given by (21)-(23), $h_2(x_1, x_2, r(t)) = k_3 W_T x^* w^* - k_4 W_T x^{**}(1 - w^*) - k_6 x^{**}$, $s(x_2, d, v) = -k_{on} p_T x^{**}(1 - c) + k_{off}(p_T/X_T)c$, $B = 1$ and $D = -X_T/p_T$. Making $T = p_T/X_T$ and $P = 1$ we have $z = Tv + Px_2$ and system (20)-(25) can now be rewritten in the form of (13) that explicitly shows the integral action given by the z dynamics as follows:

$$\dot{u}_T = \bar{k}(t) - \delta u_T \tag{26}$$

$$\dot{z} = k_3 W_T x^* w^* - k_4 W_T x^{**}(1 - w^*) - k_6 x^{**} \tag{27}$$

$$\dot{u}^* = -k_1 W_T u^*(1 - w^*) + k_2 W_T w^*(u_T - u^*) + k_p(u_T - u^*) - k_p' u^* - \delta u^* \tag{28}$$

$$\dot{w}^* = k_1 U_0 u^*(1 - w^*) - k_2 U_0 w^*(u_T - u^*) + k_4 X_T x^*(1 - w^*) - k_3 X_T \left(1 - x^* - x^{**}\right) w^* - k_3 X_T x^* w^* + k_4 X_T x^{**}(1 - w^*) - k_7 w^* \tag{29}$$

$$\dot{x}^* = k_3 W_T \left(1 - x^* - x^{**}\right) w^* - k_4 W_T x^*(1 - w^*) - k_3 W_T x^* w^* + k_4 W_T x^{**}(1 - w^*) - k_5 x^* + k_6 x^{**} \tag{30}$$

$$\dot{x}^{**} = k_3 W_T x^* w^* - k_4 W_T x^{**}(1 - w^*) - k_6 x^{**} - k_{on} p_T x^{**}\left(1 - T^{-1}(z - x^{**})\right) + k_{off} \frac{p_T}{X_T} T^{-1}(z - x^{**}). \tag{31}$$

This system fits the structure given in (1)-(5), with the same choice of state variables, $g_1(x_1, x_2, z, r, \beta)$ given by (27), $g_2(x_1, x_2, z, r, \beta)$ defined by (28)-(30), $g_3(x_1, x_2, z, r) = (-k_p' u^* - \delta u^*, -k_7 w^*, -k_5 x^*)'$ and $f(x_1, x_2, z, r, d, \beta)$ defined by (31). To demonstrate how Theorem 1 applies to this system, we will show that all assumptions A1-A5 are

satisfied. To this end, let us define the constants: $\alpha := k_p' + \delta$, $\beta := k_4 W_T$, $c_1 := k_1/k_4$, $c_2 := k_2/k_4$, $c_3 := k_3/k_4$, $c_5 := k_5/\alpha$, $c_6 := k_6/\beta$, $c_7 := k_7/\alpha$, $\kappa_p := k_p/\beta$, $\rho := X_T/W_T$, $\kappa_{on} := k_{on} p_T/(k_4 W_T)$, and $\kappa_{off} := k_{off} p_T/(k_4 W_T X_T)$ and re-write system (26)-(31) as:

$$\dot{u}_T = k(t) - \delta u_T \tag{32}$$

$$\dot{z} = \beta[c_3 x^* w^* - c_6 x^{**} - x^{**}(1 - w^*)] \tag{33}$$

$$\begin{aligned}\dot{u}^* = \beta[&-c_1 u^*(1 - w^*) + c_2 w^*(r - u^*) + \kappa_p(r - u^*)] \\ &- \alpha u^*\end{aligned} \tag{34}$$

$$\begin{aligned}\dot{w}^* = \beta[&c_1(U_0/W_T)u^*(1 - w^*) - c_2(U_0/W_T)w^*(r - u^*) \\ &- c_3\rho\,(1 - x^* - x^{**})\,w^* + \rho x^{**}(1 - w^*) \\ &+ \rho x^*(1 - w^*) - c_3\rho x^* w^*] - \alpha c_7 w^*\end{aligned} \tag{35}$$

$$\begin{aligned}\dot{x}^* = \beta[&c_3\,(1 - x^* - x^{**})\,w^* - x^*(1 - w^*) \\ &- c_3 x^* w^* + x^{**}(1 - w^*) + c_6 x^{**}] - \alpha c_5 x^*\end{aligned} \tag{36}$$

$$\begin{aligned}\dot{x}^{**} = \beta[&c_3 x^* w^* - c_6 x^{**} - x^{**}(1 - w^*) \\ &- \kappa_{on} x^{**}(1 - T^{-1}(z - x^{**})) + \kappa_{off} T^{-1}(z - x^{**})].\end{aligned} \tag{37}$$

For showing that assumption A1 is satisfied, we defined $\alpha := \max\{\bar{k} + \delta,\ k_p' + \delta,\ k_5,\ k_7\}$ based on the parameters shown in Fig. 3. We can see that assumption A2 is satisfied in system (32)-(37) with $\beta = k_4 W_T$ and $\bar{g}_i$, $\bar{f}$ defined from (33)-(37). For A4 we need to prove that $\mathrm{Re}[\lambda\{A\}] < 0$ uniformly in (r, d) where

$$A = \frac{\partial}{\partial(x_1, x_2, z)} \begin{pmatrix} \bar{g}_1(x_1, x_2, r) \\ \bar{g}_2(x_1, x_2, r) \\ \bar{f}_1(x_1, x_2, z, r, d) \end{pmatrix}. \tag{38}$$

To this end, the Jacobian A of system (32)-(37) was numerically evaluated for $0 \leq u_T \leq 1$ with nominal parameters and eigenvalues given in Fig. 3. Here we see that all eigenvalues have strictly negative real part, and the real part of the largest eigenvalue is bounded above by -0.58. Thus all assumptions from Theorem 1 are met and we can claim that result (1) holds for system (32)-(37), so that the trajectory of x^{**} should be independent from the load p_T applied by the downstream system.

To explicitly show how the fast internal dynamics of the YPD1/SKN7 system allow to employ integral action in order to attenuate the output disturbance and track the input signal, system (32)-(37) was simulated for decreased values of β. We can see in Fig. 4 that for ten times smaller β, the output tracking property of the YPD1/SKN7 system is impaired. Thus, the system relies on timescale separation between the input and the internal system dynamics to achieve disturbance attenuation.

IV. Conclusion and Discussion

In this paper, we have illustrated how biomolecular systems can implement a combination of integral feedback and time scale separation in order to track input stimuli while attenuating loading effects. This work hence extends the results of [16] and provides a novel interpretation for the structure of natural signal transduction networks. The mechanism for disturbance attenuation that incorporates an integral action and a fast system dynamics was shown to attenuate disturbances and to produce a tracking error that decreases as the derivative of the disturbance and reference signal decrease. This is an energy-efficient way to ensure modularity in view of unknown and varying contexts in which a system has to operate. This is especially important for engineering disciplines, such as synthetic biology, in which researchers are pursuing a bottom-up modular approach to create sophisticated new biomolecular circuits in living organisms. In particular, this work suggests that phosphorelay systems may be good candidates in synthetic biology for the design of insulation devices, which will potentially cover a role similar to that of unity gain buffers in electronics. An insulation device that exploits integral action was built and successfully implemented in yeast [35], demonstrating the applicability and relevance of the presented theoretical result.

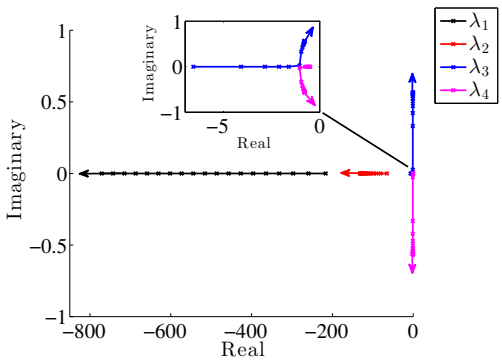

Fig. 3: The eigenvalues of the Jacobian in (38) were numerically calculated for $0 \leq u_T \leq 1$. The systems eigenvalues have strictly negative parts, with the slowest eigenvalue upper bounded by -0.58. All parameter values for this and all simulations were taken inside their allowable physical range [31], [29], [32], [33] and are summarized as follows: $\delta = 0.0065$ min^{-1}, $k_p = 1$ min^{-1}, $k_p' = 0.0533$ min^{-1}, $k_1 = 500.19$ [μM min]$^{-1}$, $k_2 = 1260$ [μM min]$^{-1}$, $k_3 = 478.85$ [μM min]$^{-1}$, $k_4 = 60$ [μM min]$^{-1}$, $k_5 = 0.01$ min^{-1}, $k_6 = 1$ min^{-1}, $k_7 = 0.01$ min^{-1}, $k_{on} = 6$ [μM min]$^{-1}$, $k_{off} = 0.0138$ min^{-1}, $X_T = 0.0712$ μM, $W_T = 0.1752$ μM.

V. Appendix

1) Example 1: Let us first define an error term $e_r(t) := r(t) - x(t)$, from (10) we have $\dot{e}_r = -k e_r - d(t)$. Integrating directly the linear system we have the solution $e_r(t) = e^{-k(t-t_0)} e_r(0) + \int_{t_0}^{t} e^{-k(t-s)}(-d(s))ds$. Using the bound $|d(t)| \leq D$ we have: $\|x(t) - r(t)\| \leq \|x(0) - r(0)\| e^{-k(t-t_0)} + (1 - e^{-k(t-t_0)})\frac{D}{k}$.

2) Example 2: Let us define the error term $e_r(t) := r(t) - x(t)$. From (11) we have that $\ddot{e}_r = -11k\dot{e}_r - 10k^2 e_r - \dot{d}$. We can define a state vector $\zeta = (e_r, \dot{e}_r)'$ and write the system in state space form $\dot{\zeta} = \begin{pmatrix} 0 & 1 \\ -10k^2 & -11k \end{pmatrix}\zeta + \begin{pmatrix} 0 \\ -1 \end{pmatrix}\dot{d}(t)$. The system has eigenvalues $\lambda_1 = -k$, $\lambda_2 = -10k$ and

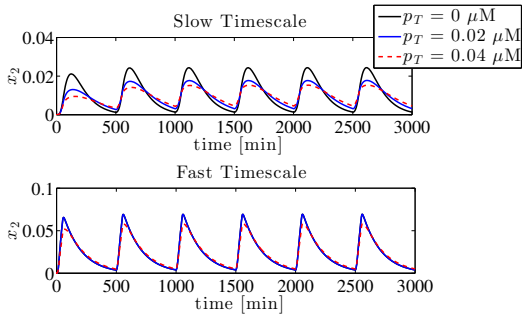

Fig. 4: System (32)-(37) was simulated under different timescales. The fast timescale corresponds to $\beta = k4W_T$ with parameter values as provided in Fig. 3, and the slow timescale simulation corresponds to decreasing the parameter β by 10. In both plots $p_T = 0$ represents the case with no downstream system (load), while the $p_T = 0.02, 0.04$ μM provide the system with increasing amounts of load. A load value of $p_T = 0.04$ corresponds to having aproximately 360 plasmids with 4 binding sites each, a number of downstream targets so large that can affect normal cell growth [34]. The considered input was a periodic square wave system inductions with a fixed on-time of 50 minutes a period of 500 minutes and magnitude of 1e-4 μM/min.

eigenvectors $v_1 = (1, -k)'$, $v_2 = (1, -10k)'$. Defining the eigenvalue matrix $\Lambda := \text{diag}\{\lambda_1, \lambda_2\}$, eigenvector matrix $V := (v_1, v_2)$ and input matrix $B := (0, -1)'$, by direct integration we have that $\zeta(t) = Ve^{\Lambda(t-t_0)}V^{-1}\zeta(0) + \int_{t_0}^{t} Ve^{\Lambda(t-s)}V^{-1}B\dot{d}(s)ds$. Using the bound $|\dot{d}(t)| \leq \alpha$ we have that $\|\zeta(t)\| \leq \|Ve^{\Lambda(t-t_0)}V^{-1}\zeta(0)\| + \left\| \begin{matrix} \frac{(1-e^{-k(t-t_0)})}{9k^2} - \frac{(1-e^{-10k(t-t_0)})}{90k^2} \\ \frac{(1-e^{-k(t-t_0)})}{9k} - \frac{(1-e^{-10k(t-t_0)})}{9k} \end{matrix} \right\| \alpha$. Thus, we have that the permanent error $\|r(t) - x(t)\| \leq \frac{\alpha}{9k^2}$.

REFERENCES

[1] K. Zhou, J. Doyle, and K. Glover. *Robust and Optimal Control*. Prentice Hall, 1996.

[2] H. Khalil. *Nonlinear Systems*. Prentice Hall, 2002.

[3] P. Kokotovic, H. K. Khalil, and J. O'Reilly. *Singular Perturbation Methods in Control*. SIAM, 1999.

[4] K. Åström and R. M. Murray. *Feedback Systems*. Princeton, 2008.

[5] C. I. Byrnes, F. D. Priscoli, and A. Isidori. *Output regulation of uncertain nonlinear systems*. Birkhauser, 1997.

[6] T-M Yi, Huang Y, M. I. Simon, and J. Doyle. Robust perfect adaptation in bacterial chemotaxis through integral feedback control. *Proc. National Academy of Science USA*, 97:46494653, 2000.

[7] L.H. Hartwell, J.J. Hopfield, S. Leibler, and A.W. Murray. From molecular to modular cell biology. *Nature*, 402:47–52, 1999.

[8] U. Alon. Network motifs: theory and experimental approaches. *Nature*, 8:450–461, June 2007.

[9] D. A. Lauffenburger. Cell signaling pathways as control modules: complexity for simplicity? *Proc. Natl. Acad. Sci.*, 97(10):5031–5033, May 2000.

[10] P. E. M. Purnick and R. Weiss. The second wave of synthetic biology: from modules to systems. *Nature Reviews Molecular Cell Biology*, 10:410–422, 2009.

[11] D. Del Vecchio, A. J. Ninfa, and E. D. Sontag. Modular cell biology: Retroactivity and insulation. *Molecular Systems Biology*, 4:161, 2008.

[12] P. Jiang, A. C. Ventura, E. D. Sontag, A. J. Ninfa, and D. Del Vecchio. Load-induced modulation of signal transduction networks. *Science Signaling*, 4:ra67, 2011.

[13] S. Jayanthi, K. Nilgiriwala, and D. Del Vecchio. Retroactivity controls the temporal dynamics of gene transcription. *ACS Synthetic Biology*, page To Appear, 2013.

[14] E. Franco, E. Friedrichs, J. Kim, R. Jungmann, R. Murray, E. Winfree, and F. C. Simmel. Timing molecular motion and production with a synthetic transcriptional clock. *Proc. Natl. Acad. Sci*, doi: 10.1073/pnas.1100060108, 2011.

[15] Y. Kim, Z. Paroush, K. Nairz, E. Hafen, G. Jiménez, and S. Y. Shvartsman. Substrate-dependent control of mapk phosphorylation in vivo. *Mol. Sys. Biol.*, 7:467, 2011.

[16] S. Jayanthi and D. Del Vecchio. Retroactivity attenuation in biomolecular systems based on timescale separation. *IEEE Trans. Aut. Control*, 56:748–761, 2011.

[17] K. D. Young, P. V. Kokotovic, and V. I. Utkin. A singular perturbation analysis of high-gain feedback systems. *IEEE Trans. Aut. Control*, AC 22(6):931–938, 1977.

[18] J. Mei-Yeh Lu, R. J. Deschenes, and J. S. Fassler. *Saccharomyces cerevisiae* histidine phosphotransferase ypd1p shuttles between the nucleus and cytoplasm for sln1-dependent phosphorylation of ssk1p and skn7p. *Eukaryotic Cell*, 2(1):13041314, 2003.

[19] S. Li, S. Dean, Z. Li, J. Horecka, J. J. Deschenes, and J. S. Fassler. The eukaryotic two-component histidine kinase sln1p regulates och1 via the transcription factor, skn7p. *Molecular biology of the cell*, 13(2):412–424, 2002.

[20] J. Huang and W. J. Rugh. On a nonlinear multivariable servomechanism problem. *Automatica*, 26(6):963–972, 1990.

[21] K. D. Young. Disturbance decoupling by high gain feedback. *IEEE Trans. Aut. Control*, AC 27(4):970–971, 1982.

[22] A. Saberi. Output-feedback control with almost-disturbancedecoupling propertya singular perturbation approach. *Int. Journal of Control*, 45(5):1705–1722, 2010.

[23] S. Oh and H. K. Khalil. Nonlinear output-feedback tracking using high-gain observer and variable structure control. *Automatica*, 33(10):1845–1856, 1997.

[24] E. Klipp, R. Herwig, A. Kowald, C. Wierling, and H. Lehrach. *Systems Biology in Practice*. Wiley-VCH, 2005.

[25] U. Alon. *An introduction to systems biology. Design principles of biological circuits*. Chapman-Hall, 2007.

[26] J. M. Rohwer, N. D. Meadow, S. Roseman, H. V. Westerhoff, and P. W. Postma. Understanding glucose transport by the bacterial phosphoenolpyruvate: glycose phosphotransferase system on the basis of kinetic measurements in vitro. *Journal of Biological Chemistry*, 275(45):34909–34921, 2000.

[27] J. E. Niven and S. B. Laughlin. Energy limitation as a selective pressure on the evolution of sensory systems. *Journal of Experimental Biology*, 211(11):1792–1804, 2008.

[28] M. T. Laub and M. Goulian. Specificity in two-component signal transduction pathways. *Annu. Rev. Genet.*, 41:121–145, 2007.

[29] E. Klipp, B. Nordlander, R. Krüger, P. Gennemark, and S. Hohmann. Integrative model of the response of yeast to osmotic shock. *Nature biotechnology*, 23(8):975–982, 2005.

[30] P. M. Rivera and D. Del Vecchio. Retroactivity attenuation through signal transduction cascades. In *American Control Conference (ACC), 2014*, pages 3387–3392. IEEE, 2014.

[31] A. Belle, L. Tanay, A.and Bitincka, and E. K. Shamir, R.and O'Shea. Quantification of protein half-lives in the budding yeast proteome. *Proceedings of the National Academy of Sciences of the United States of America*, 103(35):13004–9, August 2006.

[32] Ty. M. Thomson, K. R. Benjamin, A. Bush, T. Love, D. Pincus, O. Resnekov, R. C. Yu, A. Gordon, A. Colman-Lerner, D. Endy, and R. Brent. Scaffold number in yeast signaling system sets tradeoff between system output and dynamic range. *Proceedings of the National Academy of Sciences of the United States of America*, 108(50):20265–70, December 2011.

[33] M. Schlosshauer and D. Baker. Realistic protein-protein association rates from a simple diffusional model neglecting long-range interactions, free energy barriers, and landscape ruggedness. *Protein science: a publication of the Protein Society*, 13(6):1660–9, June 2004.

[34] S. Lin-Chao, W.T. Chen, and T.T. Wong. High copy number of the puc plasmid results from a rom/rop-suppressible point mutation in rna ii. *Molecular microbiology*, 6(22):3385–3393, 1992.

[35] D. Mishra, P. Rivera-Ortiz, D. Del Vecchio, and R. Weiss. A load driver device for engineering modularity in biological networks. *Nature Biotechnology*, 2014 to appear.